The EMBO Journal Vol.17 No.13 pp.3597–3607, 1998

Aut2p and Aut7p, two novel microtubule-associated proteins are essential for delivery of autophagic vesicles to the vacuole

Thomas Lang, Elke Schaeffeler, Daniela Bernreuther, Monika Bredschneider, Dieter H.Wolf and Michael Thumm[1]

Universität Stuttgart, Institut für Biochemie, Pfaffenwaldring 55, 70569 Stuttgart, Germany

[1]Corresponding author
e-mail: thumm@po.uni-stuttgart.de

***AUT2* and *AUT7*, two novel genes essential for autophagocytosis in the yeast *Saccharomyces cerevisiae* were isolated. *AUT7* was identified as a low copy suppressor of autophagic defects in *aut2-1* cells. Aut7p is a homologue of the rat microtubule-associated protein (MAP) light chain 3 (LC3). Aut2p and Aut7p interact physically. Aut7p is attached to microtubules via Aut2p, which interacts with tubulins Tub1p and Tub2p. *aut2*- and *aut7*-deleted cells are unable to deliver autophagic vesicles and the precursor of aminopeptidase I to the vacuole. Double membrane-layered autophagosome-like vesicles accumulate in the cytoplasm of these cells. Our findings suggest that microtubules and an attached protein complex of Aut2p and Aut7p are involved in the delivery of autophagic vesicles to the vacuole.**

Keywords: Aut2p/Aut7p/autophagocytosis/autophagosomes/LC3/microtubules

Introduction

Eukaryotic cells constitutively deliver their intracellular contents to the vacuole (or lysosome) for degradation. For the delivered proteins this is a non-specific process called autophagocytosis and it is stimulated significantly during nutrient deprivation (for reviews see Dunn, 1994; Mortimore *et al*., 1996; Seglen *et al*., 1996; Codogno *et al*., 1997). Autophagocytosis involves the formation of autophagosomes, which are vesicles containing cytoplasm typically surrounded by two membrane layers, that appear in the cytoplasm. In mammalian cells autophagosomes acquire lysosomal hydrolases very rapidly, usually within 15 min (Dunn, 1990), probably by fusing with pre-existing lysosomes and they mature to become degradative autolysosomes (Lawrence and Brown, 1992; Dunn, 1994).

In the yeast *Saccharomyces cerevisiae* the outer membrane layer of autophagosomes fuse with the vacuolar membrane, releasing autophagic vesicles into the vacuole, where they are lysed. This lysis is dependent on the active vacuolar proteinase yscB (Baba *et al*., 1994). During starvation in the presence of the proteinase yscB inhibitor phenylmethylsulfonyl fluoride (PMSF), accumulation of autophagic vesicles inside the vacuole can be visualized by light microscopy (Straub *et al*., 1997). This has made the monitoring of autophagy very simple. Also a phenotypic and genetic overlap between autophagy and the selective transport of the precursor of aminopeptidase I from the cytoplasm to the vacuole, with a half-life of ~45 min (Klionsky *et al*., 1992), has been detected (Harding *et al*., 1996). Thus, blocking aminopeptidase I precursor maturation, which occurs in almost all *aut*-mutant cells, suggests an additional way of following autophagic defects in cells.

In wild-type yeast cells autophagosomes can only rarely be detected in the cytoplasm (Baba *et al*., 1994; our unpublished results), a phenomenon probably due to the fact that they are readily taken up into the vacuole. The rapid fusion of autophagosomes with the lysosome (vacuole) suggests a directed movement of the vesicles rather than diffusion. Indeed, Aplin *et al*. (1992) reported the accumulation of acidic late autophagosomes lacking hydrolytic enzymes in mammalian cells when treated with nocodazole, a microtubule-depolymerizing drug. They speculated that autophagosomes move along the microtubular network to reach the lysosomes. Also treatment with vinblastine, a microtubule inhibitor, leads to the accumulation of autophagosomes (Seglen *et al*., 1996).

So far, however, no direct evidence for the attachment of autophagosomes to microtubules, or the proteins involved, has been obtained. Microtubules in *S.cerevisiae* consist of two α-tubulins, Tub1p and Tub3p, and the β-tubulin Tub2p (for reviews see: Solomon, 1991; Winsor and Schiebel, 1997).

To achieve a molecular understanding of the autophagic process, we isolated *aut*-mutant strains defective in autophagy (Thumm *et al*., 1994). Two genes, *AUT1* (Schlumpberger *et al*., 1997) and *AUT3* (Straub *et al*., 1997), have already been characterized.

Here we report on the identification of *AUT2* and its low copy suppressor *AUT7*, two genes essential for autophagocytosis. Aut7p has significant homology to light chain 3 (LC3), a rat microtubule-associated protein. Aut2p exhibits a direct protein–protein interaction with Tub1p, Tub2p and Aut7p. In *aut2*- and *aut7*-deleted cells autophagosome-like vesicles become detectable. Our results suggest Aut2p and Aut7p are involved in the attachment of autophagosomes to microtubules for delivery to the vacuole.

Results

Selection of an autophagocytosis-defective mutant

The *aut2-1* mutant strain, FIM39, has been identified after ethyl methanesulfonate mutagenesis as an autophagocytosis-defective mutant. This is due to its inability to degrade cytosolic fatty acid synthase and to accumulate autophagic vesicles in the presence of PMSF inside the

vacuole during starvation for nitrogen (Thumm *et al*., 1994).

Isolation of the AUT2 gene

Homozygous *aut2-1* diploid cells show a drastically reduced sporulation frequency. Following a previously described procedure (Schlumpberger *et al*., 1997), we used this phenotype to isolate the *AUT2* gene by complementation with a Ycp50-based genomic library (Rose *et al*., 1987). Screening of ~30 000 transformants yielded plasmid Ycp50/27 (Figure 1A), which in homozygous *aut2-1* mutant cells cured not only the sporulation deficiency but also the accumulation defect of autophagic vesicles in the vacuole during starvation in the presence of PMSF. In addition the defect in maturation of the precursor of aminopeptidase I was complemented by this plasmid in *aut2-1* mutant cells (Figure 3A, lane 6). Subcloning of the 6.5 kb genomic insert of Ycp50/27 identified a 1.8 kb *Xba*I–*Bcl*I-fragment (Figure 1A) sufficient for complementation. Sequencing localized this fragment to chromosome XIV. *YNL223w* was the single complete open reading frame (ORF). Chromosomal integration of the *Xba*I–*Bcl*I-fragment into *aut2-1* mutant cells followed by crossing with a wild-type strain and subsequent tetrad dissection confirmed the identity of *YNL223w* (DDBJ/EMBL/GenBank accession No.U20390) with *AUT2*. *AUT2* encodes a protein consisting of 506 amino acids (Figure 1B), with an estimated molecular mass of 56.6 kDa and an isoelectric point of ~4.5. Aut2p shares some homology with *ZK792.1* (Wilson *et al*., 1994), an ORF of unknown function from *Caenorhabditis elegans*, and with regions of tubulin α-chains of other organisms, for example α2-tubulin from maize (Figure 1C).

AUT2 is essential for the autophagic process, but not for growth

An *aut2* chromosomal null mutant was constructed, by using a PCR-based deletion method and the plasmid pUG6 (Güldener *et al*., 1996) to replace the complete ORF with a *LoxP–Kan*^{R}*–LoxP* cassette (Wach *et al*., 1994) generating canamycin resistance. Correct gene replacement was confirmed by Southern blot analysis (not shown). *Aut2*Δ cells grow as the wild-type on rich medium at 16, 30 and

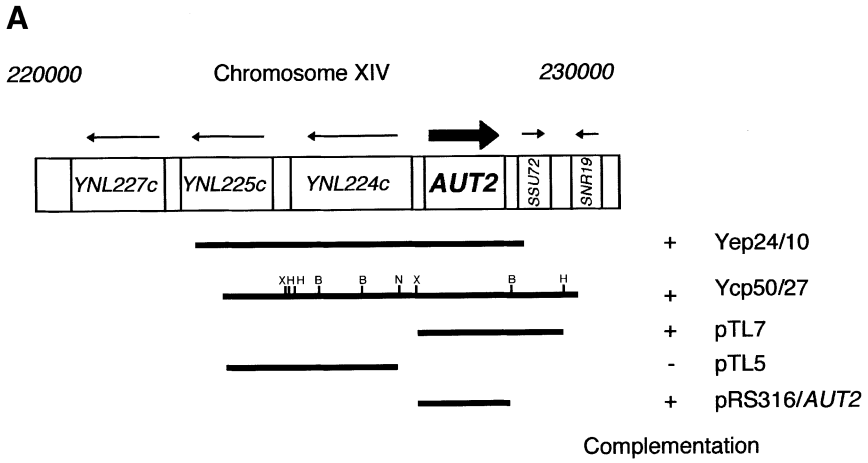

B

```
MDDFLSRIGVIYMQRWLQLWKMDLVQKVSHGVFEGSSEEPAALMNHDYIV  50
LGEVYPERDEESGAEQCEQDCRYRGEAVSDGFLSSLFGREISSYTKEFLL 100
DVQSRVNFTYRTRFVPIARAPDGPSPLSLNLLVRTNPISTIEDYIANPDC 150
FNTDIGWGCMIRTGQSLLGNALQILHLGRDFRVNGNESLERESKFVNWFN 200
DTPEAPFSLHNFVSAGTELSDKRPGEWFGPAATARSIQSLIYGFPECGID 250
DCIVSVSSGDIYENEVEKVFAENPNSRILFLLGVKLGINAVNESYRESIC 300
GILSSTQSVGIAGGRPSSSLYFFGYQGNEFLHFDPHIPQPAVEDSFVESC 350
HTSKFGKLQLSEMDPSMLIGILIKGEKDWQQWKLEVAESAIINVLAKRMD 400
DFDVSCSMDDVESVSSNSMKKDASNNENLGVLEGDYVDIGAIFPHTTNTE 450
DVDEYDCFQDIHCKKQKIVVMGNTHTVNANLTDYEVEGVLVEKETVGIHS 500
PIDEKC                                               506
```

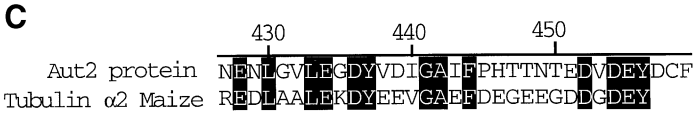

Fig. 1. (**A**) *AUT2* is identical to *YNL223w*. Genomic fragments of complementing plasmids and constructed subclones are illustrated. X, *Xba*I; B, *Bcl*I; N, *Nru*I; H, *Hin*dIII. (**B**) Protein sequence of Aut2p. (**C**) Aut2p shows weak similarities to part of tubulin α2 from maize (Montoliu *et al*., 1990).

37°C, respectively (not shown). *Aut2*Δ cells exhibit all phenotypes found for other *aut*-mutant strains analyzed so far. As expected *aut2*Δ cells were unable to accumulate autophagic vesicles in the vacuole (Figure 2A). While in *aut2-1* mutant cells some mature aminopeptidase I can be detected (Figure 3A, lane 5), in *aut2*Δ cells maturation of aminopeptidase I precursor was completely impaired (Figure 3B, lane 3). The most prominent phenotype of *aut*-mutants is their lack of starvation-induced protein breakdown (Schlumpberger *et al*., 1997; Straub *et al*., 1997). Similar to *pep4*Δ (*pra1*Δ) cells, which are impaired in vacuolar proteolytic breakdown, *aut2*Δ cells exhibited only about one third of the total protein breakdown rate found in wild-type cells (Figure 2B). Also the survival rate during starvation for nitrogen was significantly reduced in *aut2*Δ cells as compared with wild-type cells (Figure 2C).

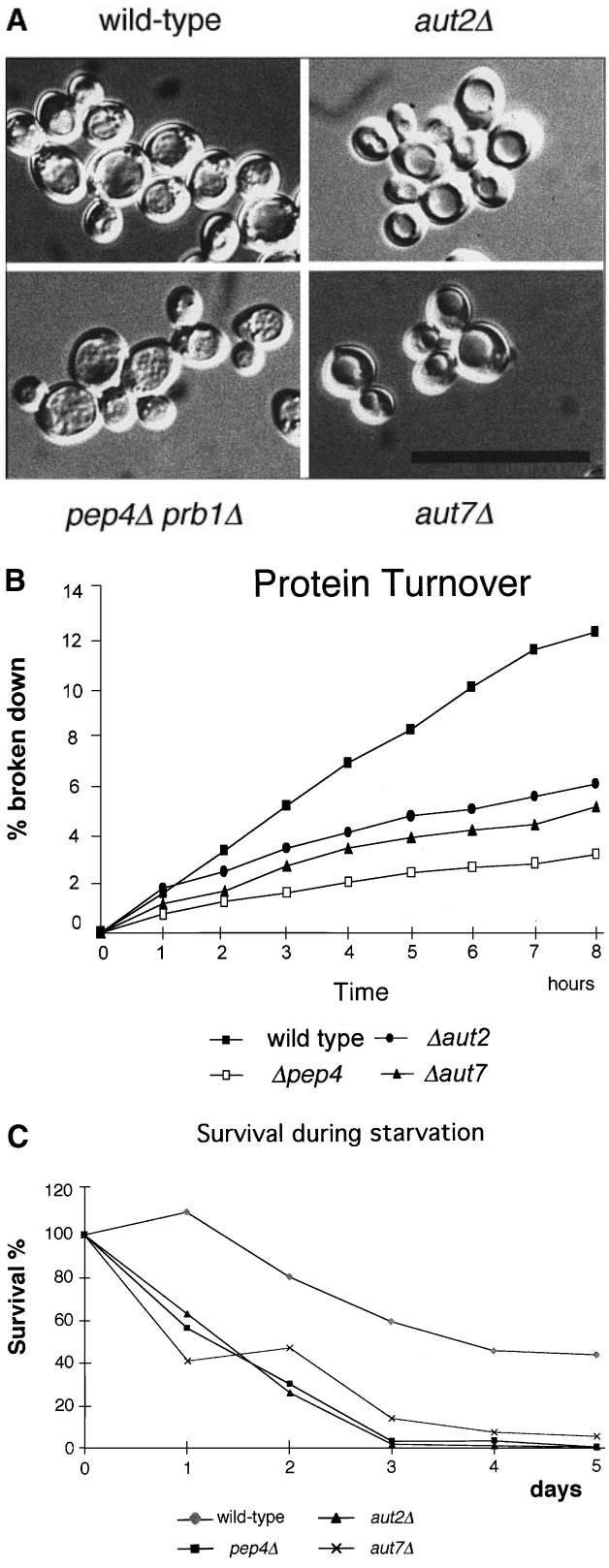

Fig. 2. (**A**) After 4 h of starvation in 1% K-acetate medium in the presence of PMSF, autophagic vesicles can be visualized in vacuoles of wild-type and *pep4*Δ *prb1*Δ cells using Normaski optics. In *aut2*Δ and *aut7*Δ cells no autophagic vesicles can be seen. Bar represents 20 μm. (**B**) Total protein breakdown of cells starved on nitrogen-free medium is significantly reduced in *aut2*Δ and *aut7*Δ cells compared with wild-type cells. *pep4*Δ (*pra1*Δ) cells are almost completely impaired in starvation-induced vacuolar protein breakdown. Cells were pulse-labeled with [^{35}S]methionine and chased on non-radioactive starvation medium. Aliquots were taken at the indicated times and acid soluble small peptides generated by proteolysis were determined according to Straub *et al*. (1997). (**C**) Survival during starvation. Like *pep4*Δ (*pra1*Δ) cells, which are almost completely impaired in vacuolar proteolysis, *aut2*Δ and *aut7*Δ cells exhibit a significantly reduced survival rate during starvation on nitrogen-free medium as compared with wild-type cells. Aliquots of cells incubated in 1% K-acetate were plated and growing colonies were determined according to Straub *et al*. (1997).

Isolation of ORF YBL078c (AUT7), an extragenic suppressor of aut2-1 mutant phenotypes: another gene essential for autophagy

To identify additional components of the autophagic pathway, we screened for high copy suppressors of the sporulation defect of homozygous diploid *aut2-1* mutant cells. Out of 50 000 transformants from an overexpressing Yep24-based genomic library, four independent plasmids Yep24/10, Yep24/24, Yep24/29 and Yep24/34 were isolated, which complemented the sporulation defect. Partial sequencing demonstrated the identity of the insert in Yep24/10 with the *AUT2* gene. The other three genomic inserts could be localized to chromosome II (Figure 4A). ORF *YBL078c* (*YBH8*) was common to all fragments and subcloning of this DNA as a *Stu*I–*Sna*BI-fragment (Figure 4A) revealed its ability to complement the maturation defect of the aminopeptidase I precursor (Figure 3A, lane 9) and the vesicle accumulation defect seen in *aut2-1* mutant cells (not shown).

As complementation of the *aut2-1* mutation also occurred with a centromeric version of *YBL078c* (DDBJ/EMBL/GenBank accession No. Z35839) or even after chromosomal integration (Figure 3A, lanes 1 and 8), we assume a very close interaction of Aut2p and Aut7p. *YBL078c* (*AUT7*) could not substitute completely for *AUT2*; in *aut2*Δ cells no suppression was observed (Figure 3B, lanes 6 and 7).

Chromosomal deletion of *YBL078c* (*AUT7*) by integrating a *LoxP–Kan^R–LoxP* cassette (Wach *et al*., 1994; Güldener *et al*., 1996), did not influence growth on rich media at 16, 30 and 37°C, respectively (not shown). Deletion was confirmed by Southern analysis (not shown).

AUT7 (YBL078c) is essential for autophagy

Aut7-deleted cells show all the phenotypes of autophagocytosis mutants. When *aut7*Δ (*ybl078c*Δ) cells were subjected to nitrogen starvation in the presence of PMSF, no

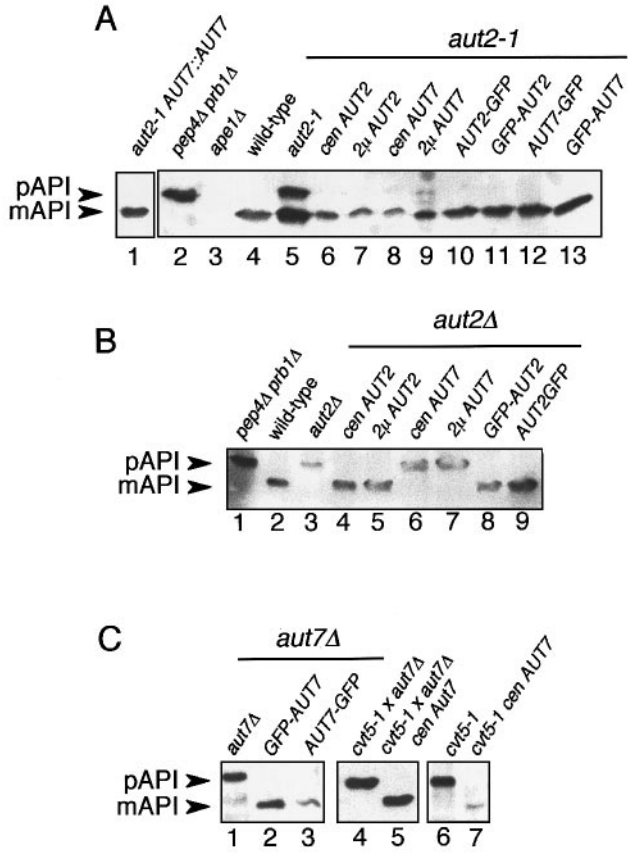

Fig. 3. Maturation of proaminopeptidase I is impaired in *aut2-1* (**A**), *aut2*Δ (**B**) and *aut7*Δ (**C**) cells. Further details are outlined in the text. Crude extracts were prepared from cells starved 4 h on 1% K-acetate.

accumulation of autophagic vesicles inside the vacuole was observed (Figure 2A). Also maturation of the aminopeptidase I precursor (Figure 3C), starvation-induced protein breakdown (Figure 2B) and the survival rate during starvation (Figure 2C) were significantly affected in these cells. We therefore named this ORF *AUT7*.

Recently a phenotypic and genetic overlap between *aut*-mutants, defective in autophagy, and *cvt*-mutants impaired in the selective cytoplasm-to-vacuole targeting (cvt) of the aminopeptidase I precursor has been described (Harding *et al*., 1996). We therefore checked for an allelism of *aut7*Δ cells with *cvt*-mutant strains (Harding *et al*., 1995, 1996). Interestingly, heterozygously defective *cvt5-1 aut7*Δ diploid cells showed only the aminopeptidase I precursor (Figure 3C, lane 4). This mutant phenotype was complemented by a plasmid borne *AUT7* gene (Figure 3C, lane 5). *cvt5-1* itself is allelic with *apg8*-mutant strains, which are defective in autophagy (Scott *et al*., 1996).

Aut7p has significant homology to the microtubule-associated rat LC3 protein

AUT7 encodes a protein of 117 amino acids with an estimated molecular mass of ~14 kDa and a predicted isoelectric point of ~9.3. Aut7p exhibits a striking homology to proteins from a variety of organisms. It shows 77% identity to the 'symbiosis-related protein' from *Laccaria bicolor*, 71% identity to AC002387 from *Arabidopsis thaliana*, 56% identity to a ganglioside expression factor-2 (GEF-2) protein from *Rattus norvegicus*, 53% identity to U23511 from *C.elegans* (Wilson *et al*., 1994), 50% identity to Z97341 from *A.thaliana*, and 28% identity to the microtubule-associated protein 1 LC3 from *R.norvegicus* (Kuznetsov and Gelfand, 1987; Mann and Hammarback, 1994, 1996) (Figure 4B).

Protein–protein interactions between Aut2p and Aut7p, Aut2p and Tub1p, and Aut2p and Tub2p

The homology of Aut7p with a microtubule-associated mammalian protein and the strong genetic interaction of *aut2-1* and *AUT7* prompted us to search for a possible protein–protein interaction between these proteins and the yeast tubulin proteins Tub1p and Tub2p. A yeast two-hybrid system with *HIS3* and *LacZ* as reporter genes was used for this search (Fields and Song, 1989; Fields and Sternglanz, 1994). Sole expression of fusion constructs of the *GAL4* activator and binding domain did not result in any staining indicating that no protein–protein interaction occurred (not shown). In contrast, strong interactions were detected between Aut2p and Aut7p, Aut2p and Tub1p, and Aut2p and Tub2p (Figure 5A), as indicated by formation of the blue reaction product of X-Gal after 3 h incubation at 30°C.

Confirmation of the protein–protein interactions detected with the two-hybrid system, was performed by protein affinity chromotography. A glutathione-*S*-transferase–Aut2p (GST–Aut2p) fusion protein was bound to a glutathione affinity column. We incubated this GST–Aut2p column with a crude extract of *aut7*Δ cells expressing a biologically active C-terminal fusion protein of Aut7p with the 'Green Fluorescent Protein' (GFP) (Aut7p–GFP-C). After washing with 500 mM NaCl, proteins bound were eluted and analyzed using antibodies directed against GFP. As expected, Aut7p–GFP was bound to the GST–Aut2p affinity column (Figure 5B, lane 3). When GST alone was bound to the column, as a control, no Aut7p–GFP became bound (Figure 5B, lane 6).

Bovine tubulin has been found to interact with yeast tubulin-associated proteins similar to yeast tubulin (Barnes *et al*., 1992). To confirm the binding of tubulin to Aut2p, we therefore incubated a GST–Aut2p column with bovine tubulin. As shown in Figure 5C, lane 12, bovine tubulin was found attached to the GST–Aut2p column even after washing with buffer containing NaCl. If GST alone was bound to the column no bovine tubulin became bound (lane 9). Protein staining with Coomassie indicate the presence of GST–Aut2p and tubulin (lane 6).

Two-hybrid analysis indicated no direct interaction between Aut7p and tubulin. We also analyzed binding of bovine tubulin to a GST–Aut7p column. As with GST alone, no bound tubulin was detected in this experiment (Figure 5D, lanes 9 and 12). Coomassie staining demonstrated the presence of GST–Aut7p in the eluate fraction (Figure 5D, lane 6). In lane 3 GST is visible. When binding very large amounts of GST–Aut7p to the column, a very faint band, becomes visible (not shown). We consider this faint band not to be due to a specific binding of Aut7p to bovine tubulin.

aut2Δ and aut7Δ cells are not sensitive to benomyl

Benomyl is a microtubule-depolymerizing drug. Altered sensitivity (i.e. hypersensitivity or resistance) to benomyl is an indication for a change in microtubule stability

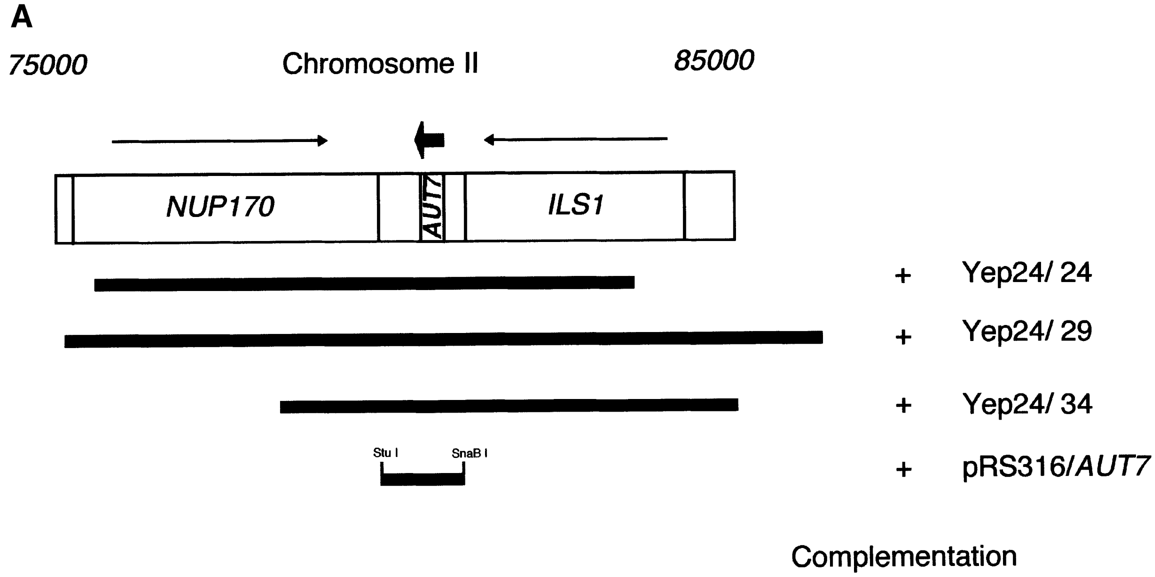

B

```
                         10        20
1   -----------MKSTFKSEYPFEKRKAESERIADRFKNRI  Aut7p
1   --------MPSEK-TFKQRRSFEQRVEDVRLIREQHPTKI  LC3 rat
1   DQISITHAVSTMRSKFKDEHPFEKRKAEAERIRQKYPDRI  Laccaria bicolor U93506
1   N---------------------------------------  A.thaliana AC002387
1   -----------MKWMFKEDHSLEHRCVESAKIRAKYPDRV  GEF-2 protein
1   -----------MKWAYKEENNFEKRRAEGDKIRRKYPDRI  U23511 C.elegans
1   -----------------------KRRAEAARIREKYPDRI  Z97341 A.thaliana

    30        40        50        60
30  PVICEK-AEKSDIPEIDKRKYLVPADLTVGQFVYVIRKRI  Aut7p
32  PVIIERYKGEKQLPVLDKTKFLVPDHVNMSELIKIIRRRL  LC3 rat
41  PVICEK-ADRTDIPTIDKKKYLVPSDLTVGQFVYVIRKRI  Laccaria bicolor U93506
2   SVIVEK-AEKSEVPNIDKKKYLVPSDLTVGQFVYVIRKRI  A.thaliana AC002387
30  PVIVEK-VSGSQIVDIDKRKYLVPSDITVAQFMWIIRKRI  GEF-2 protein
30  PVIVEK-APKSKLHDLDKKKYLVPSDLTVGQFYFLIRKRI  U23511 C.elegans
18  PVIVEK-AEKSDIPTIDKKKYLVPADLTVGQFVYVIRKRI  Z97341 A.thaliana

    70        80        90        100
69  MLPPEKAIFIFVN-DTLPPTAALMSAIYQEHKDKDGFLYV  Aut7p
72  QLNANQAFFLLVNGHSMVSVSTPISEVYESERDEDGFLYM  LC3 rat
80  KLAPEKAIFIFVD-EVLPPTAALMSAIYEEHKDEDNFLYV  Laccaria bicolor U93506
41  KLSAEKAIFIFVD-NVLPPTGELMSSVYEDKKDEDGFLYI  A.thaliana AC002387
69  QLPSEKAIFLFVD-KTVPQSSLTMGQLYEKEKDEDGFLYV  GEF-2 protein
69  QLRPEDALFFFVN-NVIPQTMTTMGQLYQDHHEEDLFLYI  U23511 C.elegans
57  KLSAEKAIFIFVD-NVLPPAGKQIDLLCIQDSG----VSL  Z97341 A.thaliana

     110
108 TYSGENTFGR                                Aut7p
112 VYASQETFGT------------------------------  LC3 rat
119 SYSGENTFGQEGWVELPVDDMDKAFICVSAAKKHWVWVLC  Laccaria bicolor U93506
80  TYSGENTFGASS----------------------------  A.thaliana AC002387
108 AYSGENTFG-------------------------------  GEF-2 protein
108 AYSDESVYGGE-------------------VEKKE       U23511 C.elegans
92  SFNTSNK--SIRRRLLICSPVRSCLLC---TKRKRMMMGS  Z97341 A.thaliana

117                                           Aut7p
122 ALAVTYMSA-LKATATGRE------------------PCL  LC3 rat
159 DVRSSYQNCVLIVPLVQRPVLHTHSSFLSVSFALLF---V  Laccaria bicolor U93506
92  ---------------------------------------I  A.thaliana AC002387
117 ---------------------------------------F  GEF-2 protein
123                                           U23511 C.elegans
127 SMSLTAEKTHLDLDLHNRDLLL-DISFYSSLFSPNISSSY  Z97341 A.thaliana
```

Fig. 4. (**A**) *AUT7* is identical to *YBL078c*. Genomic fragments isolated from an overexpression library and leading to suppression of the autophagic defects in *aut2-1* mutant cells are illustrated. A complementing *Stu*I–*Sna*BI subclone carrying only *AUT7* as a complete ORF was constructed.
(**B**) Homologues of Aut7p. Sequences were aligned using the Clustal method. Residues identical with Aut7p are shaded in black. Further details are given in the text.

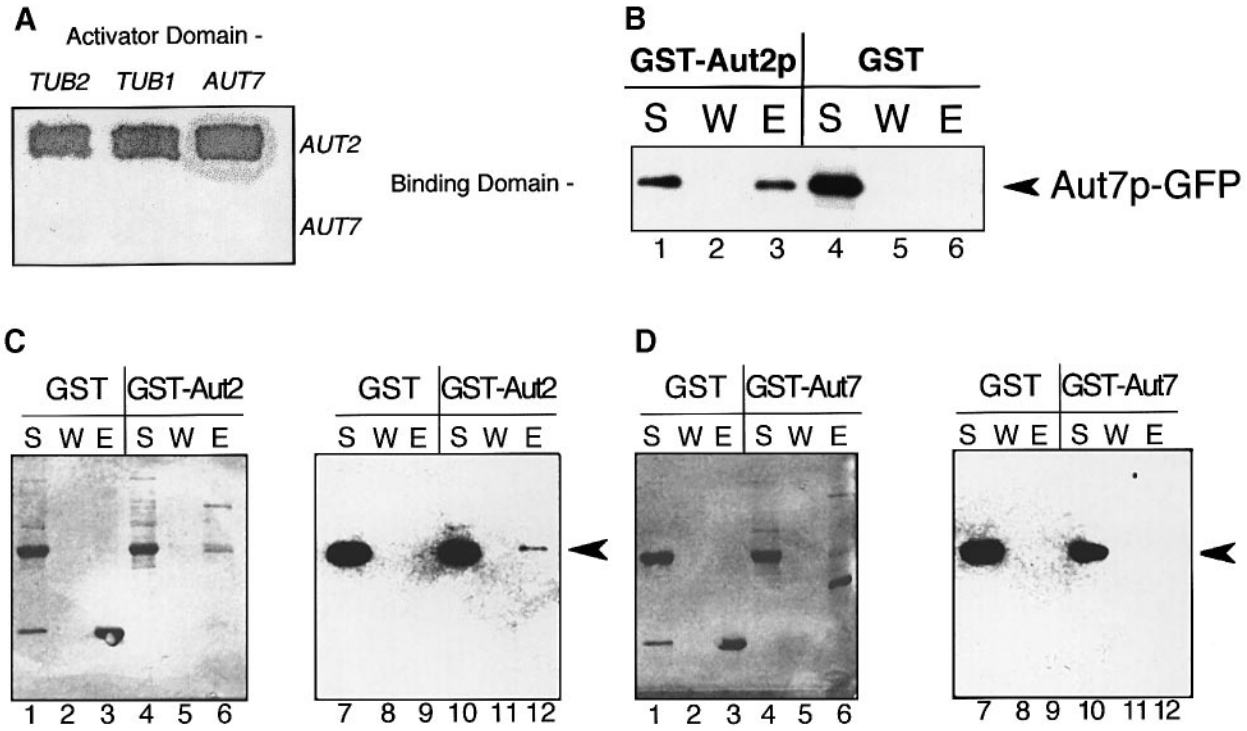

Fig. 5. (**A**) Detection of protein–protein interactions using the two-hybrid system. Intense staining indicates an interaction between Aut2p and Aut7p, Aut2p and Tub1p, and Aut2p and Tub2p. *AUT7*, *TUB1* and *TUB2* are cloned in-frame with the *GAL4*-activator domain. *AUT2* and *AUT7* were fused to the *GAL4*-binding domain (see Materials and methods). (**B**) Affinity chromatography confirms protein–protein interaction between Aut2p and Aut7p. A fusion protein of Aut2p with the 26 kDa glutathione-*S*-transferase (GST) domain from *Schistosoma japonicum* (see Materials and methods) was bound to glutathione–Sepharose 4B. This GST–Aut2p column was incubated with a crude extract from *aut7*Δ *cen Met25::AUT7–GFP* cells. The non-bound supernatant (S) fraction (lane 1) was taken away. Gel beads were successively washed with NaCl solutions of increasing concentrations to remove non-specifically bound proteins. After the final 500 mM NaCl wash (W, lane 2), bound proteins were eluted with Laemmli buffer (E, lane 3). Samples were analyzed in immunoblots with monoclonal antibodies directed against GFP. Using Aut2p–GST, a clear band corresponding to Aut7p–GFP is seen in the eluate fraction (lane 3, arrowhead). As a control, GST alone was attached to the column and no band was detectable (lane 6). (**C**) As described in (B), bovine tubulin binds to GST–Aut2p glutathione–Sepharose 4B (lane 12), but not to GST glutathione–Sepharose 4B (lane 9). Protein staining with Coomassie is shown in lanes 1–6; in lanes 7–12 tubulin was detected using monoclonal antibodies (Boehringer Mannheim). Further details are given in Materials and methods. (**D**) Similar to (C), bovine tubulin does not bind to GST–Aut7p glutathione–Sepharose 4B (lane 12) and to GST glutathione–Sepharose 4B (lane 9). Lanes 1–6, protein staining with Coomassie; lanes 7–12 probed with antibodies directed against tubulin.

(Interthal *et al*., 1995). We therefore expected that overexpression of *AUT2* or *AUT7* in wild-type cells or chromosomal deletion of *AUT2* or *AUT7* in cells would show benomyl sensitivity or resistance, if Aut2p or Aut7p were involved in modulating microtubule stability. At concentrations of 15 or 30 μg/ml no altered growth rates were detected (Figure 6) indicating a non-structural function of Aut2p and Aut7p.

Autophagosomes accumulate in starved aut2Δ and aut7Δ cells

A detailed electron microscopic analysis of *aut2*Δ and *aut7*Δ cells led to the detection of double membrane-layered vesicles with an appropriate diameter of ~170–180 nm in the cytoplasm of these cells during starvation (Figure 7A and B). The two membrane layers surrounding these vesicles can easily be seen (Figure 7B, arrowheads). Vesicular content was indistinguishable from cytoplasm (Figure 7A and B). We further confirmed the accumulation of autophagosome-like vesicles. We isolated these vesicles by modifying an established cell fractionation procedure (Harding *et al*., 1996), which used hypotonically lysed spheroplasted cells (total fraction, T), (Figure 7C, lane 3). Following this procedure with wild-type cells yielded a 6000 *g* pellet fraction (P_6, Figure 7C, lane 4) consisting of plasma membrane fragments, endoplasmic reticulum and intact vacuoles and a 6000 *g* supernatant fraction (S_6, Figure 7C, lane 5) which was almost entirely cytosolic (Harding *et al*., 1995). We introduced an additional 100 000 *g* centrifugation step, which when starting with the S_6 fraction, yielded a P_{100} pellet fraction (Figure 7C, lane 6) and a S_{100} supernatant fraction (Figure 7C, lane 7). We used cells starved for 20 h on nitrogen-free medium and followed the intracellular localization of fatty acid synthase (Fas) as a suitable cytosolic marker protein (Egner *et al*., 1993). In *pep4*Δ (*pra1*Δ) cells, exhibiting a defect in vacuolar proteolysis, due to the action of the autophagic process, part of Fas is detected in the vacuolar P_6 fraction (Figure 7C, lane 4) (Thumm *et al*., 1994; Schlumpberger *et al*., 1997). No visible P_{100} pellet was obtained in this experiment and no Fas could be detected in this fraction (Figure 7C, lane 6). In contrast, following this procedure with *aut2*Δ cells, a clearly visible P_{100} pellet was obtained, which observed under the light microscope consisted of vesicles. At the same time significant amounts of Fas could be detected in the P_{100} fraction of *aut2*Δ cells (Figure 7D, lane 7). Due to the defect in autophagocytosis, in *aut2*Δ cells, no Fas was found to be

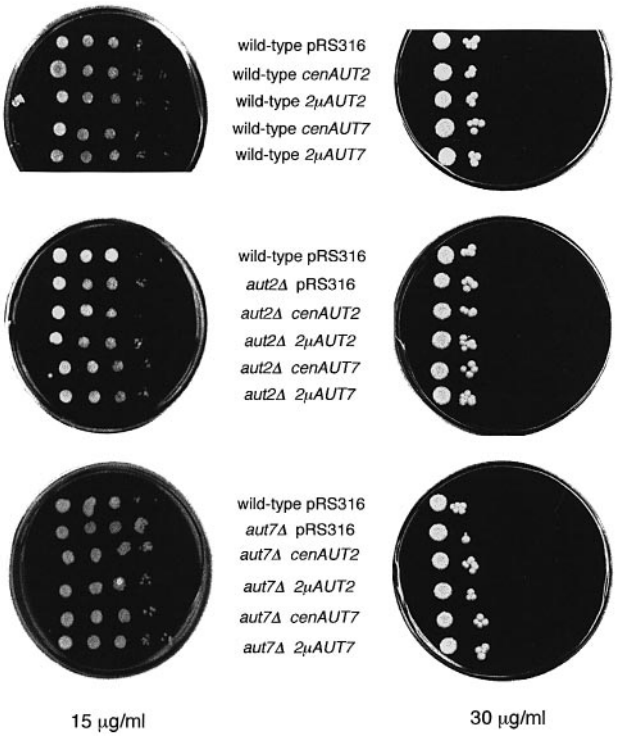

Fig. 6. Benomyl sensitivity of wild-type cells overexpressing *AUT2* and *AUT7*, and of *aut2*Δ and *aut7*Δ cells is not altered. Cells were grown to stationary phase and dilution series with decreasing cell densites were dropped on CM plates without uracil containing 15 and 30 μg/ml benomyl. Plates were incubated at 30°C.

localized in the vacuole (Figure 7D, lane 4). But proteinase K protection experiments with total fraction T in the absence and presence of Triton X-100 (Figure 7D, lane 1 and 2) demonstrate that part of Fas is membrane-protected in *aut2*Δ cells. This is a further indication for the accumulation of cytosol-containing vesicles in the cytosol of *aut2*Δ cells.

Localization of Aut2p and Aut7p

N- and C-terminal fusion proteins of Aut2p and Aut7p with the fluorescent GFP protein from *Aequorea victoria* (Cubitt *et al*., 1995; Stearns, 1995) were constructed. The constructs were placed under the control of the inducible *MET25* promotor using the plasmids pRN295 and pRN963. Expression of the fusion proteins rescued autophagic defects of the respective chromosomally deleted cells, indicating that the Aut2p–GFP and Aut7p–GFP fusion proteins were biologically active (Figure 3A, lanes 10–13; Figure 3B, lanes 8 and 9; Figure 3C, lanes 2 and 3).

Fluorescence of fusion proteins appeared unevenly distributed throughout the cytoplasm, Aut2p and Aut7p seemed to focus in some areas (not shown).

Discussion

Insight into the mechanistic principles of autophagocytosis should result from the study of a variety of previously isolated *aut*-mutants defective in autophagocytosis (Thumm *et al*., 1994). Complementation of the sporulation defect of homozygous *aut2-1* diploid cells with a genomic library was used to identify the *AUT2* gene (Figure 1). *AUT2* is not essential for growth on rich media at 16, 30 and 37°C. However *aut2*-deleted cells exhibit the phenotypes characteristic for *aut*-mutant cells (Schlumpberger *et al*., 1997; Straub *et al*., 1997). (i) They are unable to accumulate autophagic vesicles inside the vacuole during starvation for nitrogen in the presence of PMSF (Figure 2A). (ii) The total protein breakdown during starvation is significantly reduced (Figure 2B). (iii) The survival rate of mutant cells during periods of nutrient limitation is reduced (Figure 2C). (iv) The cell differentiation process of sporulation is almost completely blocked in mutant diploids (not shown). (v) The vacuolar uptake and maturation of the aminopeptidase I precursor is blocked in logarithmically growing cells and in cells starved for nitrogen (Figure 3). Aut2p is predicted to be a soluble protein with no significant homology to proteins of known function, and limited homologies to some α-tubulin chains (Figure 1C).

A screen for high copy suppressors of autophagic defects of *aut2-1* cells identified—besides *AUT2* itself—the ORF *YBL078c*. Chromosomally deleted *YBL078c* cells showed all the characteristic features of mutant strains with autophagic defects listed above (Figure 2A–C and Figure 3C), we therefore named this gene *AUT7*. *Aut7*Δ cells were found to be allelic with *cvt5-1* cells (Figure 3C). *cvt5-1* cells have been isolated for their blockage in the selective cytoplasm-to-vacuole targeting of the aminopeptidase I precursor (Harding *et al*., 1995). Interestingly they are also allelic to *apg8* mutant cells which, in an independent approach, have been isolated for their defect in autophagy (Scott *et al*., 1996). No DNA sequences have been reported for *CVT5* and *APG8* so far. Aut7p is a small protein of 13.6 kDa, which shows significant homology to some proteins of unclear biological function and to LC3, a component of microtubule-associated protein (MAP) complexes isolated from brain (Kuznetsov and Gelfand, 1987; Mann and Hammarback, 1994, 1996). LC3 has been found in ternary protein complexes associated with either MAP1A (275 kDa) or MAP1B (244 kDa) and LC1 (27 kDa) as a third protein. Another light chain LC2 (24 kDa) specifically associates with MAP1A. Electron microscopic studies suggested that these protein complexes form long filamentous arms linked to the microtubules and connecting microtubules to each other, and so possibly modulating microtubule shape (Shiomura and Hirokawa, 1987; Sato-Yoshitake *et al*., 1989; Pedrotti *et al*., 1996).

AUT7 does not only act as a suppressor of autophagic defects in *aut2-1* mutant cells in high copy number, but also in low copy number: chromosomal integration of an additional copy of *AUT7* is sufficient for suppression (Figure 3A). This indicated a possible interaction of Aut2p and Aut7p on the protein level. We therefore tried to determine a direct protein–protein interaction between Aut2p and Aut7p using the two-hybrid system. Because of the strong homology between Aut7p and the microtubule-associated LC3 protein from rat, we also included Tub1p and Tub2p as components of the yeast tubulin cytoskeleton in this analysis. We were able to detect strong interactions between Aut2p and Aut7p, Aut2p and Tub1p, and Aut2p and Tub2p. These findings suggested the formation of a protein complex consisting of Aut2p and Aut7p, which is attached to microtubules via interactions between Aut2p and Tub1p, and Aut2p and Tub2p, respectively.

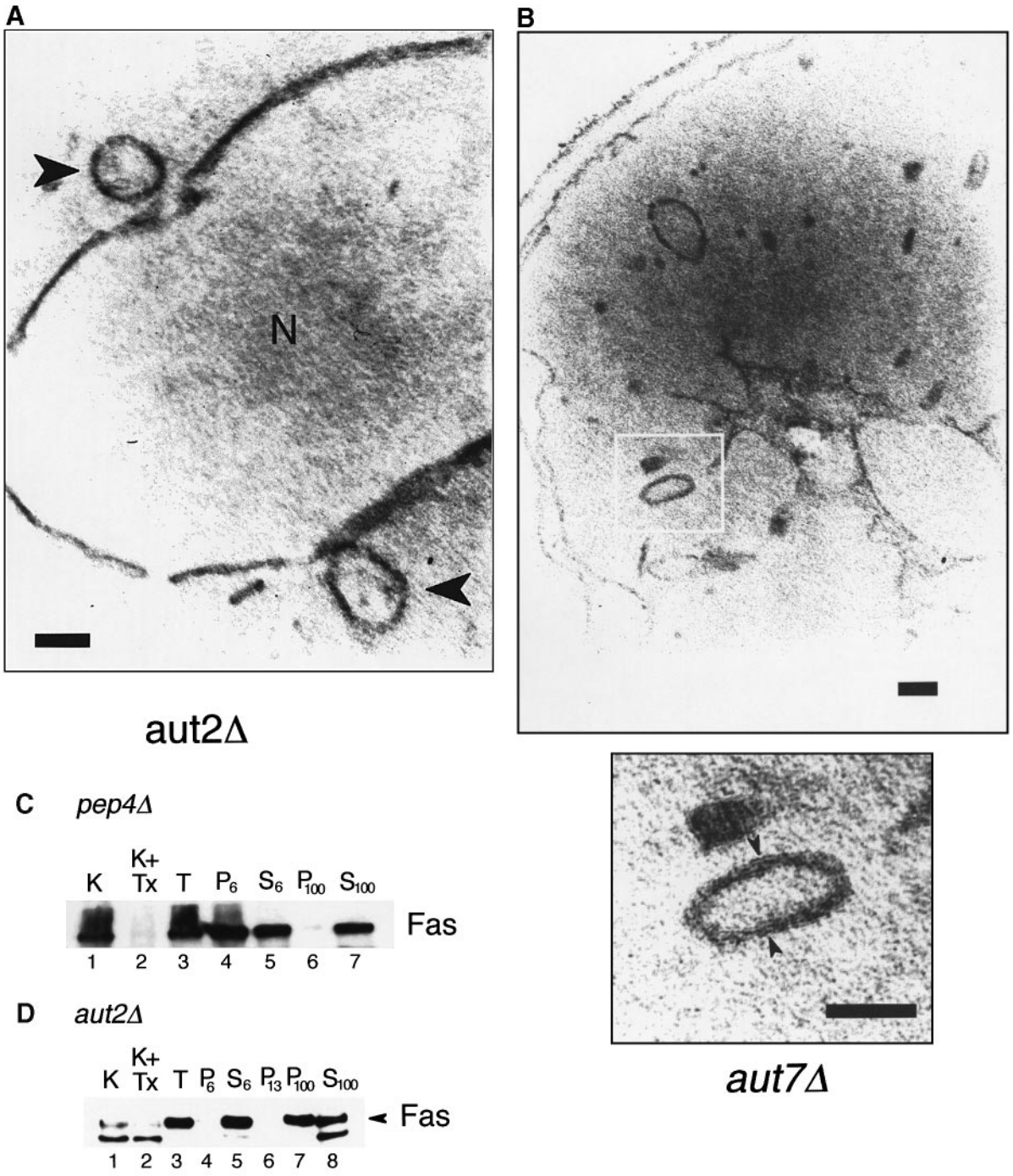

Fig. 7. (**A**) Autophagosome-like vesicles (arrowhead) are accumulating in the cytoplasm of *aut2*Δ cells starved for 4 h on 1% K-acetate in the presence of PMSF. Bar represents 100 nm. (**B**) Electron micrographs unravels the accumulation of double membrane-layered autophagosome-like vesicles in the cytoplasm of *aut7*Δ cells starved for 3 h in nitrogen-free medium in the presence of PMSF. Arrowheads indicate the clearly distinguishable two membrane layers. Bar represents 100 nm. **(C** and **D**) Cytosol containing autophagosome-like vesicles accumulating in the cytosol of *aut2*Δ cells (D) can be isolated with an additional 100 000 *g* centrifugation step yielding a P_{100} pellet fraction. In wild-type cells (C), no P_{100} is detectable. Fatty acid synthase (Fas) was used as a cytosolic protein. Further details are given in the text.

We confirmed this interaction by binding a GST–Aut2p fusion protein to an affinity column followed by incubation with a crude extract of *aut7*Δ cells expressing a biologically active Aut7p–GFP fusion protein. Indeed, after removing non-specifically bound proteins from the affinity column Aut7p could be detected (Figure 5B). Using bovine tubulin, which has been shown to be equivalent to yeast tubulin in binding yeast-associated proteins (Barnes *et al*., 1992), we demonstrate the interaction of Aut2p with tubulin (Figure 5C). With a predicted isoelectric point of 4.5, Aut2p is negatively charged at physiological pH. Aut7p on the other hand is positively charged (predicted isoelectric point 9.3). This may be relevant for formation of the Aut2p–Aut7p protein complex attached to microtubules.

In *S.cerevisiae* mutations influencing microtubule stability have been shown to cause altered sensitivity to the microtubule-depolymerizing drug, benomyl (Schatz *et al*., 1988; Interthal *et al*., 1995). Cells deleted for *aut2*

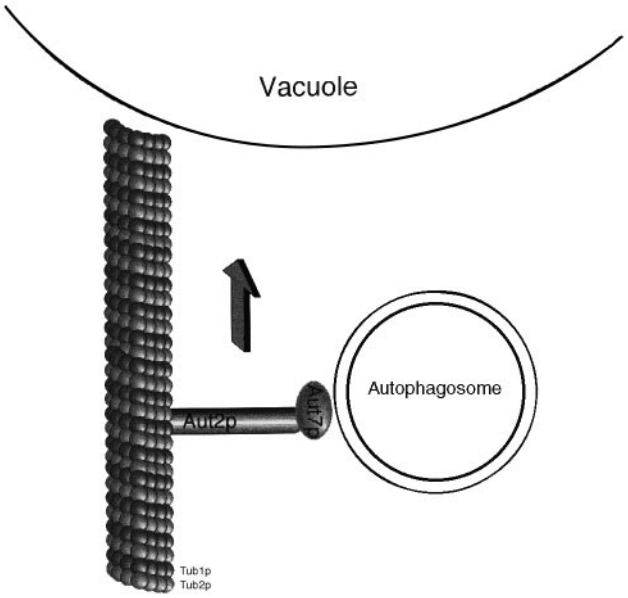

Fig. 8. Schematic illustration of how Aut2p and Aut7p are involved in the attachment of autophagosomes to microtubules allowing their directed movement to the vacuole. Aut2p interacts with Tub1p and Tub2p of microtubules.

or *aut7*, or wild-type cells overexpressing *AUT2* or *AUT7* exhibited no sensitivity or resistance to benomyl compared with wild-type cells (Figure 6). Furthermore, no cold- or temperature-sensitive phenotype is seen with *aut2*Δ or *aut7*Δ cells (not shown). This indicates that Aut2p and Aut7p in *S.cerevisiae* may not affect the stability of microtubules.

In wild-type cells autophagosomes are only rarely detectable (Baba *et al*., 1994), (Figure 7C) suggesting their rapid uptake by the vacuole. In *aut2*Δ and *aut7*Δ cells, we detected double membrane-layered autophagosome-like vesicles with a minimal diameter of 170–180 nm in the cytosol (Figure 7A, B and D). Furthermore we were able to demonstrate that in contrast to wild-type cells, part of cytoplasmic fatty acid synthase can be sedimented in a P_{100} fraction of *aut2*Δ cells. We therefore consider *aut2*Δ cells to be defective in vacuolar uptake or transport of autophagosomes.

GFP fusion proteins of Aut2p and Aut7p under control of the strong *MET25*-promotor did not appear evenly distributed in the cytoplasm (not shown).

Taken together our findings suggest the existence of a protein complex consisting of Aut7p and Aut2p which itself interacts with Tub1p and Tub2p (Figure 8). Whether additional proteins are attached to this complex or whether Aut7p directly interacts with autophagosomes has still to be determined. The detection of autophagosomes in *aut2*- or *aut7*-deficient cells support the idea that autophagosomes are attached to microtubules via Aut2p and Aut7p to achieve their rapid, directed movement towards the vacuole (Figure 8). This model would be in good agreement with the findings of Aplin *et al*. (1992), who observed the accumulation of acidic late autophagosomes lacking hydrolytic enzymes in the cytoplasm of mammalian cells after applying the microtubule-depolymerizing drug, nocodazole. Also application of vinblastine, another drug interfering with the microtubules, lead to the accumulation of autophagosomes in mammalian cells (Seglen *et al*., 1996).

Aut7p is a member of a new protein family consisting of proteins with only scarcely understood functions. They are from various organisms and include the 'symbiosis-related protein' from *L.bicolor* (77% identity), AC002387 protein from *A.thaliana* (71% identity), GEF-2 protein (56% identity) from *R.norvegicus*, U23511 protein (53% identity) from *C.elegans* (Wilson *et al*., 1994), Z97341 protein (50% identity) from *A.thaliana*, and to microtubule-associated protein 1 LC3 (28% identity) from *R.norvegicus* (Kuznetsov and Gelfand, 1987; Mann and Hammarback, 1994, 1996), (Figure 4B). LC3 from rat has been shown to bind directly to microtubules (Mann and Hammarback, 1994). Two-hybrid analysis (Figure 5A) and the use of GST–Aut7p affinity columns with bovine tubulin (Figure 5D) does not support a direct interaction of Aut7p with tubulin. We cannot exclude, however, an interaction of Aut7p with yeast tubulin *in vivo*. Interestingly, two proteins with different homologies to Aut7p has been found so far in *R.norvegicus* and in *A.thaliana*, respectively. It is conceivable that, the GEF-2 protein sharing 56% identity with Aut7p rather than LC3 with only 28% identity is the functional homologue.

Nevertheless, it is tempting to speculate that some Aut7p relatives in other organisms, might have the same or similar functions as Aut7p in *S.cerevisiae*, namely transport of vesicles along microtubules. It will be a challenging task to test this hypothesis.

Materials and methods

Chemicals and media

Yeast cells were starved in 1% K-acetate. Other media were prepared according to standard protocols (Ausubel *et al*., 1987). Chemicals were of analytical grade.

Strains

WCG4a *Mata his3-11,15 leu2-3,112 ura3* (Thumm *et al*., 1994); YMTABα *Matα his3-11,15 leu2-3,112 ura3 pra1*Δ*::HIS3 prb1*Δ (Thumm *et al*., 1994); FIM39/7b *Mata leu2-3,112 ura3 his3-11,15 aut2-1*, (backcrossed three times with WCG4) (Thumm *et al*., 1994); YTL4 *Mata his3-11,15 leu2-3,112 ura3 ade2*Δ*1 aut2-1* (this study); YTL5 *Matα Mata his3-11,15 his3-11,15 leu2-3,112 leu2-3,112 ura3 ura3 ade2 ADE2 aut2-1 aut2-1* (this study); YTL8 *Mata his3-11,15 leu2-3,112 ura3 aut2-1 AUT7::AUT7::URA3* (this study); YTL9 *Mata his3-11,15 leu2-3,112 ura3 aut2*Δ*::KAN* (this study); YTL11 *Mata his3-11,15 leu2-3,112 ura3 aut7*Δ*::KAN* (this study); DYY101 *Matα leu2-3,112 ura3-52, his3-*Δ*200 trp1-*Δ*901 lys2-801 suc2-*Δ*9* Δ*ape1::LEU2* (Harding *et al*., 1995); THY313 *Mata leu2-3,112 ura3-52 his3-*Δ*200 trp1-*Δ*901 ade2-101 suc2-*Δ*9 cvt5-1* (Harding *et al*., 1995), Y190a *Mata gal4 gal80 his3 trp1-901 ade2-101 ura3-52 leu2-3,-112 URA3::GAL* → *lacZ, LYS2:: GAL(UAS)* →*HIS3* (S.J.Elledge, Houston, USA).

YTL4 was obtained by chromosomal deletion of the *ADE2* gene in *aut2-1* mutant with a 2.3 kb *Bam*HI fragment from pPL131 (Schlumpberger *et al*., 1997). YTL8 was obtained by chromosomal integration of *Hpa*I linearized pRS306/*AUT7* in *aut2-1* mutant cells. Using oligonucleotides Δaut2 KAN1, Δaut2 KAN2 or Δaut7 KAN1; Δaut7 KAN2 and plasmid pUG6, two DNA fragments for the chromosomal replacement of *AUT2* or *AUT7* with a *LoxP–KAN^R–LoxP* cassette were created by PCR. The strains YTL9 or YTL11 were made by transforming the single *LoxP–KAN^R–LoxP* cassettes into WCG4a. Y190a was used for the two-hybrid assay, YTL5 for isolation of *AUT2* and *AUT7* according to Schlumpberger *et al*. (1997).

GST–Aut2 and GST–Aut7 fusion proteins

A *Eco*RI–*Xho*I fragment containing *AUT2* was generated by PCR using oligonucleotides GST1 AUT2, GST2 AUT2, and pRS316/*AUT2*. It was introduced in the *Eco*RI–*Xho*I site of pGEX-4T-3 (Pharmacia, Freiburg,

Germany). After inducing protein expression for 4 h with 0.1 mM isopropyl-β-D-galactopyranoside, the 82 kDa fusion protein was isolated following the manufacturer's protocol and bound to glutathione–Sepharose 4B (Pharmacia, Freiburg) during a 30 min incubation. Similarly, a *Bam*HI–*Xho*I fragment containing *AUT7* was generated using oligonucleotides (ATT ACT GGA TCC ATG AAG TCT ACA TTT AAG TCT; and TAT AAA CTC GAG CCT GCC AAA TGT ATT TTC TCC) and pRS316/*AUT7*. It was introduced into pGEX-4T-3.

Protein affinity chromatography

Twenty OD midlog cells of strain YTL11 pGFP–*AUT7* were lysed using glass beads. Crude extracts in PBS buffer (140 mM NaCl, 2.7 mM KCl, 10 mM Na_2HPO_4, 1.8 mM KH_2PO_4) were incubated overnight at 4°C with gentle shaking with GST–Aut2p (or GST) bound to glutathione–Sepharose 4B. Supernatant (S) was removed and the beads were washed successively with 50 µl each of a solution containing 15.6, 31.2, 62.5, 125, 250 and 500 mM NaCl (fraction W, wash) in PBS buffer to remove unspecifically bound proteins. After eluting all proteins (fraction E) with 50 µl Laemmli buffer, 10 µl of all fractions were analyzed in immunoblots with anti-GFP antibodies (Molecular Probes, Leiden, The Netherlands).

Bovine tubulin binding

GST–Aut2p (or GST) bound to glutathione–Sepharose 4B (~10 µl) was incubated with 30 µg bovine tubulin (Sigma, Deisenhofen) in 80 µl PEM buffer (100 mM PIPES–NaOH pH 6.6, 1 mM EGTA, 1 mM $MgSO_4$). One µl of 100 mM GTP and 0.5 µl of 10 mM Taxol was added and incubated for 10 min at 37°C. We continued as outlined above, but stopped washing at a concentration of 250 mM NaCl, and used monoclonal anti-bovine tubulin antibodies (Boehringer Mannheim, Mannheim) for detection.

Cell fractionation

Subcellular fractionation were carried out as described by Harding *et al*. (1996) with the following modifications. Cells were starved 20 h in 1% K-acetate before spheroplast formation. Unlysed cells were removed by an additional 300 *g* centrifugation step. Cytosol-enriched S_6 fraction was centrifuged for 1 h yielding a S_{100} supernatant and a P_{100} pellet fraction. Fractions were analyzed by immunoblotting with a rabbit anti-fatty acid synthase antibody (1:5000) (Thumm *et al*., 1994) and a goat anti-rabbit antibody coupled to peroxidase (Medac, Hamburg, Germany) (1:5000). Peroxidase activity was detected using the ECL-system (Amersham, Braunschweig, Germany).

Two-hybrid assay

In-frame fusions with the *GAL4* activator domain were constructed by ligating (i) a 1.5 kB *Bam*HI–*Xho*I fragment carrying *AUT2*; (ii) a 1.45 kB *Bam*HI–*Sal*I fragment carrying *TUB1* in pGAD-C1 (James *et al*., 1996), digested with *Bam*HI–*Sal*I, yielding pGAD-C1/*AUT2*, and pGAD-C1/*TUB1*, respectively. Ligation of (iii) a 1.37 kB *Sma*I–*Pst*I fragment carrying *TUB2* in the respective sites of pGAD-C1 yielded pGAD-C1/*TUB2*. DNA fragments were generated by PCR using (i) pRS316/AUT2 and oligonucleotides AUT2-2hybrid and AUT2-2hybrid1; (ii) pRB306 (D.Botstein, Stanford, CA) and oligonucleotides TUB1 and TUB1,1; (iii) pRB129 (D.Botstein, Stanford, CA) and oligonucleotides TUB2 and TUB2,1. In-frame fusions with the *GAL4* DNA-binding domain were similarly constructed by ligating (i) a 1.5 kB *Nco*I–*Sal*I fragment containing *AUT2*; (ii) a 0.35 kB *Bam*HI–*Xho*I fragment containing *AUT7* into the *Bam*HI–*Xho*I sites of pAS1-CYH2 (S.J.Elledge, Houston, USA), yielding pAS-CYH2/*AUT2* and pAS1-CYH2/*AUT7*. Also these DNA fragments were generated by PCR with (i) pRS316/*AUT2* and oligonucleotides AUT2-2hybrid and AUT2-2hybrid,1; (ii) pRS316/*AUT7* and oligonucleotides AUT7-2hybrid,2 and AUT7-2hybrid, (iii) PCR fragments were purified from agarose gels and digested with corresponding enzymes.

Plasmids pGAD-C1/*AUT2*, pAS1-CYH2/*AUT2* and pAS1-CYH2/*AUT7* were able to complement the vesicle accumulation defect of *aut2*Δ and *aut7*Δ cells, respectively, indicating biological activity.

Oligonucleotides

GFP1 AUT7 5′-ATT ACT TCT AGA ATG AAG TCT ACA TTT AAG TCT-3′; GFP2 AUT7 5′-TAT AAA AAG CTT CCT GCC AAA TGT ATT TTC TCC-3′; GFP1 AUT2 5′-AGT AGA TCT AGA ATG GAC GAC TTC TTA TCA CGT-3′; GFP2 AUT2 5′-TTC CTT AAG CTT GCA TTT TTC ATC AAT AGG ACT-3′; GST1 AUT2 5′-AGT AGA GAA TTC AAT GGA CGA CTT CTT ATC ACG T-3′; GST2 AUT2 5′-TTC CTT CTC GAG GCA TTT TTC ATC AAT AGG ACT-3′; AUT2-2Hybrid 5′-AGT AGA CCA TGG AGA TGG ACG ACT TCT TAT CAC GT-3′; AUT2-2Hybrid,1 5′-TTC CTT GTC GAC GCA TTT TTC ATC AAT AGG ACT-3′; AUT7-Hybrid 5′-ATT ACT CCA TGG AGA TGA AGT CTA CAT TTA AGT CT-3′; AUT7-2Hybrid,1 5′-TAT AAA GTC GAC CCT GCC AAA TGT ATT TTC TCC-3′; AUT7-2Hybrid,2 5′-ATT ACT GGA TCC ATG AAG TCT ACA TTT AAG TCT-3′; AUT7-2Hybrid,3 5′-TAT AAA CTC GAG CCT GCC AAA TGT ATT TTC TCC –3′; TUB1 5′-CAA ACA GGA TCC ATG AGA GAA GTT ATT AGT ATT-3′; TUB1,1 5′-TGA ACC GTC GAC AAA TTC CTC TTC CTC AGC GTA-3′; TUB2 5′-TGA ATA CCC GGG ATG AGA GAA ATC ATT CAT ATC-3′; TUB2,1 5′-ACT TAA CTG CAG TTC AAA ATT CTC AGT GAT TGG-3′; Δaut2 KAN1 5′-ATG GAC GAC TTC TTA TCA CGT ATA GGA GTG ATA TAC ATG CAG AGG CAG CTG AAG CTT CGT ACG C-3′; Δaut2 KAN2 5′-GCA TTT TTC ATC AAT AGG ACT GTG AAT ACC TAC CGT TTC CTT CTC GCA TAG GCC ACT AGT GGA TCT G-3′; Δaut7 KAN1 5′-CCT GCC AAA TGT ATT TTC TCC TGA GTA AGT GAC ATA CAA AAA CCC CAG CTG AAG CTT CGT ACG C-3′; Δaut7KAN2 5′-ATG AAG TCT ACA TTT AAG TCT GAA TAT CCA TTT GAA AAA AGG AAG GCA TAG GCC ACT AGT GGA TCT G-3′.

GFP–Aut2 and GFP–Aut7 fusion proteins

pRN295 and pRN963 (J.Hegemann, Giessen, Germany) were digested with *Xba*I–*Hin*dIII and a 1.5 kb *Xba*I–*Hin*dIII fragment containing *AUT2* was ligated in-frame, yielding pGFP-N/*AUT2* and pGFP-C/*AUT2*. The DNA fragment was generated by PCR using pRS316/*AUT2* and oligonucleotides GFP1 AUT2, GFP2 AUT2. pGFP-N/*AUT7* and pGFP-C/*AUT7* were created similarly by ligating a 0.35 kb *Xba*I–*Hin*dIII fragment containing *AUT7* in-frame into *Xba*I–*Hin*dIII of pRN295 and pRN963, respectively. The 0.35 kb DNA-fragment was also generated by PCR using pRS316/*AUT7* and oligonucleotides GFP1 AUT7, GFP2 AUT7.

Biological activity of all GFP fusion proteins were confirmed by complementation tests.

pGFP-C/*AUT2*, pGFP-N/*AUT2*, pGFP-C/*AUT7* and pGFP-N/*AUT7* were transformed in *aut2-1* mutant cells and the corresponding chromosomal null mutant strains YTL9 and YTL11. For induction of the *MET25* promotor, strains were incubated overnight in methionine-free CM medium. Localization of GFP was examined by fluorescence microscopy using a Zeiss Axioscope.

Measurement of protein turnover and survival rates during starvation, microscopy using Nomarski optics and preparation for electron microscopy using permanganate fixation and epon embedding was performed as described elsewhere (Straub *et al*., 1997).

We routinely used starvation on nitrogen-free media to induce the autophagic process.

Acknowledgements

We thank D.Botstein for providing plasmids carrying *TUB1* and *TUB2*, S.J.Elledge for supplying plasmids for the two-hybrid system. R.Y.Tsien and J.H.Hegemann for plasmids used to generate GFP fusions and deletions using Kanamycin as a marker. D.J.Klionsky provided aminopeptidase I antibodies and *cvt5-1* cells. We are grateful to A.Szallis for technical help. This work was supported by DFG, Bonn, Germany (grant Wo210/12-1) and the Fonds der Chemischen Industrie, Frankfurt, Germany.

References

Aplin,A., Jasionowski,T., Tuttle,D.L., Lenk,S.E. and Dunn,W.J. (1992) Cytoskeletal elements are required for the formation and maturation of autophagic vacuoles. *J. Cell Physiol.*, **152**, 458–466.

Ausubel,F.M., Brent,R., Kingston,R.E. and Moore,D.D. (1987) *Current Protocols in Molecular Biology*, Greene Publishing Associates, New York, NY.

Baba,M., Takeshige,K., Baba,N. and Ohsumi,Y. (1994) Ultrastructural analysis of the autophagic process in yeast: detection of autophagosomes and their characterization. *J. Cell Biol.*, **124**, 903–913.

Barnes,G., Louie,K.A. and Botstein,D. (1992) Yeast proteins associated with microtubules *in vitro* and *in vivo*. *Mol. Biol. Cell*, **3**, 29–47.

Codogno,P., Ogier-Denis,E. and Houri,J.J. (1997) Signal transduction pathways in macroautophagy. *Cell Signal*, **9**, 125–30.

Cubitt,A.B., Heim,R., Adams,S.R., Boyd,A.E., Gross,L.A. and Tsien,R.Y. (1995) Understanding, improving and using green fluorescent proteins. *Trends Biochem. Sci.*, **20**, 448–455.

Dunn,W.J. (1990) Studies on the mechanisms of autophagy: maturation of the autophagic vacuole. *J. Cell Biol.*, **110**, 1935–1945.

Dunn,W.J. (1994) Autophagy and related mechanisms of lysosome-mediated protein degradation. *Trends Cell. Biol*., **4**, 139–143.

Egner,R., Thumm,M., Straub,M., Simeon,A., Schüller,H.J. and Wolf,D.H. (1993) Tracing intracellular proteolytic pathways. Proteolysis of fatty acid synthase and other cytoplasmic proteins in the yeast *Saccharomyces cerevisiae*. *J. Biol. Chem*., **268**, 27269–27276.

Fields,S. and Song,O. (1989) A novel genetic system to detect protein–protein interactions. *Nature*, **340**, 245–246.

Fields,S. and Sternglanz,R. (1994) The two-hybrid system: an assay for protein–protein interactions. *Trends Genet.*, **10**, 286–292.

Güldener,U., Heck,S., Fielder,T., Beinhauer,J. and Hegemann,J.H. (1996) A new efficient gene disruption cassette for repeated use in budding yeast. *Nucleic Acids Res*., **24**, 2519–2524.

Harding,T.M., Morano,K.A., Scott,S.V. and Klionsky,D.J. (1995) Isolation and characterization of yeast mutants in the cytoplasm to vacuole protein targeting pathway. *J. Cell Biol*., **131**, 591–602.

Harding,T.M., Hefner-Gravink,A., Thumm,M. and Klionsky,D.J. (1996) Genetic and phenotypic overlap between autophagy and the cytoplasm to vacuole targeting pathway. *J. Biol. Chem.*, **271**, 17621–17624.

Interthal,H., Bellocq,C., Bahler,J., Bashkirov,V.I., Edelstein,S. and Heyer,W.D. (1995) A role of Sep1 (= Kem1, Xrn1) as a microtubule-associated protein in *Saccharomyces cerevisiae*. *EMBO J*., **14**, 1057–1066.

James,P., Halladay,J. and Craig,E.A. (1996) Genomic libraries and a host strain designed for highly efficient two-hybrid selection in yeast. *Genetics*, **144**, 1425–1436.

Klionsky,D.J., Cueva,R. and Yaver,D.S. (1992) Aminopeptidase I of *Saccharomyces cerevisiae* is localized to the vacuole independent of the secretory pathway. *J. Cell Biol*., **119**, 287–299.

Kuznetsov,S.A. and Gelfand,V.I. (1987) 18 kDa microtubule-associated protein: identification as a new light chain (LC-3) of microtubule-associated protein 1 (MAP-1). *FEBS Lett*., **212**, 145–148.

Lawrence,B.P. and Brown,W.J. (1992) Autophagic vacuoles rapidly fuse with pre-existing lysosomes in cultured hepatocytes. *J. Cell Sci*., **102**, 515–526.

Mann,S.S. and Hammarback,J.A. (1994) Molecular characterization of light chain 3. A microtubule binding subunit of MAP1A and MAP1B. *J. Biol. Chem*., **269**, 11492–11497.

Mann,S.S. and Hammarback,J.A. (1996) Gene localization and developmental expression of light chain 3: a common subunit of microtubule-associated protein lA (MAPlA) and MAP1B. *J. Neurosci. Res*., **43**, 535–544.

Montoliu,L., Rigau,J. and Puigdomenech,P. (1990) A tandem of alpha-tubulin genes preferentially expressed in radicular tissues from *Zea mays*. *Plant Mol. Biol*., **14**, 1–15.

Mortimore,G.E., Miotto,G., Venerando,R., and Kadowaki,M. (1996) Autophagy. *Subcell. Biochem.*, **27**, 93–135.

Pedrotti,B., Francolini,M., Cotelli,F. and Islam,K. (1996). Modulation of microtubule shape *in vitro* by high molecular weight microtubule associated proteins MAP1A, MAP1B, and MAP2. *FEBS Lett.*, **384**, 147–150.

Rose,M.D., Novick,P., Thomas,J.H., Botstein,D. and Fink,G.R. (1987) A *Saccharomyces cerevisiae* genomic plasmid bank based on a centromere-containing shuttle vector. *Gene*, **60**, 237–243.

Sato-Yoshitake,R., Shiomura,Y., Miyasaka,H. and Hirokawa,N. (1989) Microtubule-associated protein 1B: molecular structure, localization, and phosphorylation-dependent expression in developing neurons. *Neuron*, **3**, 229–238.

Schatz,P.J., Solomon,F. and Botstein,D. (1988) Isolation and characterization of conditional-lethal mutations in the TUB1 alpha-tubulin gene of the yeast *Saccharomyces cerevisiae*. *Genetics*, **120**, 681–695.

Schlumpberger,M., Schaeffeler,E., Straub,M., Bredschneider,M., Wolf,D.H. and Thumm,M. (1997) AUT1, a gene essential for autophagocytosis in the yeast *Saccharomyces cerevisiae*. *J. Bacteriol.*, **179**, 1068–1076.

Scott,S.V., Hefner-Gravink,A., Morano,K.A., Noda,T., Ohsumi,Y. and Klionsky,D.J. (1996) Cytoplasm-to-vacuole targeting and autophagy employ the same machinery to deliver proteins to the yeast vacuole. *Proc. Natl Acad. Sci. USA*, **93**, 12304–12308.

Seglen,P.O., Berg,T.O., Blankson,H., Fengsrud,M., Holen,I. and Stromhaug,P.E. (1996) Structural aspects of autophagy. *Adv. Exp. Med. Biol.*, **389**, 103–111.

Shiomura,Y. and Hirokawa,N. (1987) The molecular structure of microtubule-associated protein 1A (MAP1A) *in vivo* and *in vitro*. An immunoelectron microscopy and quick-freeze, deep-etch study. *J. Neurosci.*, **7**, 1461–1469.

Solomon,F. (1991) Analyses of the cytoskeleton in *Saccharomyces cerevisiae*. *Annu. Rev. Cell Biol*., **7**, 633–662.

Stearns,T. (1995) Green fluorescent protein. The green revolution. *Curr. Biol.*, **5**, 262–264.

Straub,M., Bredschneider,M. and Thumm,M. (1997) AUT3, a serine/threonine kinase gene, is essential for autophagocytosis in *Saccharomyces cerevisiae*. *J. Bacteriol.*, **179**, 3875–3883.

Thumm,M., Egner,R., Koch,B., Schlumpberger,M., Straub,M., Veenhuis,M. and Wolf,D.H. (1994) Isolation of autophagocytosis mutants of *Saccharomyces cerevisiae*. *FEBS Lett.*, **349**, 275–280.

Wach,A., Brachat,A., Pohlmann,R. and Philippsen,P. (1994) New heterologous modules for classical or PCR-based gene disruptions in *Saccharomyces cerevisiae*. *Yeast*, **10**, 1793–1808.

Wilson,R. *et al*. (1994) 2.2 Mb of contiguous nucleotide sequence from chromosome III of *C. elegans*. *Nature*, **368**, 32–38.

Winsor,B. and Schiebel,E. (1997) Review: an overview of the *Saccharomyces cerevisiae* microtubule and microfilament cytoskeleton. *Yeast*, **13**, 399–434.

Received February 9, 1998; revised April 20, 1998; accepted April 23, 1998